THESIS FOR THE DEGREE OF DOCTOR OF PHILOSOPHY

Influences of temperature, fatigue and mixed mode loading on the cohesive properties of adhesive layers

by

Tomas Walander

Department of Applied Mechanics

CHALMERS UNIVERSITY OF TECHNOLOGY

Gothenburg, Sweden 2015

Influences of temperature, fatigue and mixed mode loading on the cohesive properties of adhesive layers

TOMAS WALANDER
Gothenburg, 2015
ISBN 978-91-7597-185-8

tomas.walander@gmail.com

THESIS FOR THE DEGREE OF DOCTOR OF PHILOSOPHY
Doktorsavhandlingar vid Chalmers tekniska högskola
Ny serie nr. 3866
ISSN 0346-718X

Department of Applied Mechanics
Chalmers University of Technology
SE-412 96 Gothenburg
Sweden
Telephone: +46 (0)31-772 1000

Chalmers Reproservice
Gothenburg, Sweden 2015

Influences of temperature, fatigue and mixed mode loading on the cohesive properties of adhesive layers

TOMAS WALANDER
Department of Applied Mechanics
CHALMERS UNIVERSITY OF TECHNOLOGY

Abstract

This thesis concerns some aspects that have influence on the strength of adhesive layers. The strength is determined by the stress deformation-relation of the layer. This relation is also referred to as cohesive law. The aspects having influence on the cohesive laws that are studied in this work are *temperature, fatigue, multi-axial fatigue* and *mixed mode loading.*

For each aspect, a model is developed that can be used to describe the influence of the aspects on the cohesive laws numerically, e.g. by using the finite element method. These models are shown to give good agreement with the experimental results when performing simulations that aims at reproducing the experiments. For the aspect of temperature, a FE-model is suggested that can be used to simulate the mechanical behaviour in pure mode loadings at any temperature within the evaluated temperature span. Also, a damage law for modelling high cycle fatigue in a bonded structure in multi-axial loading is presented. Lastly, a new experimental set-up is presented for evaluating strength of adhesives during mixed mode loading. The set-up enables loading with a constant mode-mix ratio and by the experimental results, a potential model for describing the mechanical behaviour of the evaluated adhesive is presented.

Keywords: adhesive layer, cohesive law, fatigue, finite element analysis, fracture energy, mixed mode, multi-axial fatigue, potential model, temperature.

Preface

This work has been carried out during the years 2010 and 2015 at the department of Mechanics of Materials at the University of Skövde, Sweden.

Firstly, I would like to thank my supervisor Professor Ulf Stigh and my co-supervisor Anders Biel for their help and valuable inputs.

I also like to acknowledge my co-authors and colleagues at Fraunhofer IFAM in Bremen and Scania CV in Södertälje for their extensive interest and effort in our common work and to all of my present and former colleagues, at various departments at the University of Skövde, for making such a nice atmosphere.

Finally, my deepest gratitude to my family and friends for their understanding, engagement and enthusiasm - especially to my dear Kristina and our precious daughter Saga that makes me long to go home when I am at work.

Skövde, March 2015

Tomas Walander

List of appended papers

This thesis is based on the combined work in the following four papers:

- Paper A:
  T. Walander, A. Biel and U. Stigh (2013). *Temperature dependence of cohesive laws for an epoxy adhesive in Mode I and Mode II loading*. Int J Frac, 183:203-21.

- Paper B:
  A. Eklind, **T. Walander**, T. Carlberger, U. Stigh (2014) *High cycle fatigue crack growth in Mode I of adhesive layers - Modelling, simulation and experiments*. Int J Frac, 190:125-146

- Paper C:
  T. Walander, A. Eklind, T. Carlberger, U. Stigh, A. Rietz: Title: *Fatigue life of adhesively bonded structures*. Submitted.

- Paper D:
  T. Walander, S. Marzi, O. Hesebeck: *Controlled mixed-mode bending tests to determine cohesive laws of structural adhesive layers*. Submitted.

Contribution to co-authored papers

All four papers are prepared in collaboration with co-authors. The contribution by the author of this thesis is listed below:

- **Paper A:**
  Planned and wrote the paper.
  Responsible for parts of the theoretical developments.
  Planned and performed the experiments together with one of the co-authors.
  Evaluated the experiments.
  Responsible for the simulations.
  Responsible for the verifications.

- **Paper B:**
  Planned and wrote the paper together with two of the co-authors.
  Planned the experiments together with the co-authors.
  Performed the experiments together with one of the co-authors.
  Evaluated the experiments together with one of the co-authors.
  Together with one of the authors responsible for the simulations.
  Together with one of the authors responsible for the verifications.

- **Paper C:**
  Planned and wrote the paper together with the co-authors.
  Planned the experiments together with the co-authors.
  Performed the experiments together with one of the co-authors.
  Evaluated the experiments together with one of the co-authors.

- **Paper D:**
  Planned and wrote the paper.
  Primary responsible for the theoretical developments.
  Developed and build the test-set-up together with the co-authors.
  Planned and performed the experiments together with one of the co-authors.
  Evaluated the experiments.
  Responsible for the verifications.

Table of contents

To Saga
Daddy and mommy loves you

Review and summary of thesis

1. Background

With the use of adhesives, the performance of a structure can be optimized, e.g. by enabling joining of lightweight and high-strength materials. As an example, by using adhesives combinations of lightweight and tough materials can be considered in order to obtain lighter and more durable structures. Traditionally joining in structures, are performed by welding and/or rivets. Welding has the disadvantage that it cannot easily join metals having dissimilar melting temperatures. Also the solidification process of a weld gives rise to micro cracks and pre-stresses that shorten the lifetime of a welded joint. Joining of dissimilar materials can be performed using rivets and also advanced welding techniques have been developed for this purpose. However problems with galvanic corrosion may occur if, for example, steel and aluminium are joined. This in particular if the structure is used in a Nordic climate.

Usage of adhesives for joining of structures has a number of advantages over other techniques, but it also has a number of drawbacks and disadvantages. In comparison to rivets and welding, adhesives have the benefit that they can be distributed over a large area, with a thickness that is adjustable to the mismatches in shape of the counterparts that are bonded. Further, the adhesive layer insulates and seals between the materials and by this, galvanic corrosion are avoided. As is shown by the results in this thesis, the strength of some adhesives is high enough to be able to be used for highly load carrying structures. One of the disadvantages with adhesives is that bonded structures cannot be disassembled without destructing the adhesive layer. Also, some types of adhesives need both time and heat to cure and might be sensitive to ultraviolet light and to elevated temperatures.

To test structures experimentally by the use of destructive test methods is often an ineffective method that is associated with high costs. One main reason is the fact that it is time-consuming to prepare and perform the experiments. Another reason for the high costs is that several, nominally identical, experiments need to be performed in order to get reliable results. This is since experimental results contain scatter. As a substitution, or complement, of full-scale experimental tests it is more cost efficient to analyse a structure using the finite element method (FEM). This becomes obvious when several modifications and variants need to be tested and/or where the manufacturing cost is high for each tested component.

2. Introduction

The benefits with adhesives have led to that the automotive industry has attracted focus to both the usage and numerical simulations of adhesive layers in body structures. By this, knowledge about, and the ability to simulate, fracture and strength of adhesively bonded structures plays a major role in the development of complex bonded structures. The fracture characteristics and the strength of adhesive layers have been investigated in many studies. From these studies, the strength of bonded joints is shown to depend on several aspects. Examples of such aspects are listed as:

- thickness of the adhesive layer, cf. e.g. Kinloch and Shaw (1981), Chai (2004), Lee et al. (2004), Pardoen et al. (2005), Ji et al. (2010) and Marzi et al. (2014)
- the strain rate of which the adhesive is loaded to fracture, cf. e.g. Chai (2004), Marzi et al. (2009), Carlberger et al. (2009), Cho et al. (2012), and May et al. (2015)
- the curing time of the adhesive, cf. e.g. Sadr et al. (2007) and Cadenaro et al. (2009)

- the width of the adhesive layer, cf. e.g. Schnell et al. (1998) and Biel et al. (2012)
- effects of plasticity in the adherends or in the adhesive, cf. e.g. Evans et al. (1999), Lane et al. (2000), Yang and Thouless (2001a), Yang and Thouless (2001b) and Crocombe et al. (2006)
- the surface treatments and/or roughness of the bonded surfaces, cf. e.g. Mostovoy et al. (1971), Fuller et al. (1975), Wingfield (1993), Suliman et al. (1993), Persson and Tosatti (2001), Lucena-Martín et al. (2001), Uehara and Sakurai (2002), Vieira et al. (2004), Persson et al. (2005) and Atsu et al. (2006).

The studies presented in **Papers A** to **D** in this thesis are focused on the influence in strength on some of such aspects and are aimed as a continuation and/or contribution to the work in the previous studies. The studied aspects are *temperature*, *mixed mode* loading, *fatigue* loading and *mixed mode fatigue* loading of adhesive layers. Mixed mode fatigue loading is also referred to as multi-axial fatigue.

All of these aspects have been studied previously but with different aims and adhesives. The influence of temperature on the strength of adhesive layers is studied previously in e.g. Li and Jiao (2000), Chai (2004), Carlberger et al. (2009) and Banea et al. (2012). The studies by Li et al. (2000) and Banea et al. (2012) report the influence of temperature on Young's modulus of the studied adhesives. In Carlberger et al. (2009), it is shown that the cohesive laws for an epoxy adhesive is temperature dependent in Mode I loading for temperatures below the glass transition temperature. No previous study on the temperature dependence of cohesive laws in Mode II loading has been reported and the work performed in this thesis is thus the first to report this.

Fatigue of adhesive layers is studied experimentally in both pure mode and mixed mode loadings by e.g. Lee et al. (1991), Kinloch and Osiyemi (1993), Pirondi and Moroni (2009), Abdel Wahab et al. (2010a), Abdel Wahab et al. (2010b). Models to predict or simulate fatigue damage are presented by e.g. Abdel Wahab et al. (2002), Khoramishad et al. (2010a) and Khoramishad et al. (2010b). The theory that is developed in **Paper B** is inspired by the theory in Pirondi and Nicoletto (2004) and Graner Solana et al. (2010).

Mixed mode loading to fracture of adhesive layers is also studied extensively. One essential parameter having a major influence on the resistance against failure of bonded structures is the fracture energy of the adhesive layer. Several experimental studies have evaluated the influence of mode-mix on the fracture energy. Examples of such studies are Charalambides et al. (1992), Stamoulis et al. (2014), Parvatareddy and Dillard (1999), Álvarez et al. (2013) and Conroy et al. (2013). Methods to determine cohesive laws in mixed mode loadings are suggested by e.g. Lundsgaard-Larsen et al. (2008), Sørensen and Kirkegaard (2006), Sørensen and Jacobsen (2009) and Högberg et al. (2007). Models for simulations of adhesive layers during mixed mode loading are presented in e.g. Benzeggagh and Kenane (1996), Högberg (2006) and Salomonsson and Andersson (2010) and a review of such models is given by Park and Paulino (2011).

The disposition of this brief introduction is constructed so that the used definition of loading modes and cohesive laws of an adhesive layer are firstly given. Then a brief description of the used theory and the used test specimens for determining cohesive laws of an adhesive are presented. The introduction ends with a presentation of the concepts of fatigue and high cycle fatigue.

Cohesive laws in pure mode loading

An illustration of an adhesive layer bonding two adherends is shown in Fig. 1. The assembly, consisting of the adhesive layer and the adherends, are frequently denoted an adhesive system. An applied force F is acting on the system, resulting in deformations in the adhesive layer. Klarbring

(1991) and Schmidt (2008) show by asymptotic analyses that a thin linearly elastic adhesive layer of a compliant material can be considered to be exposed to two main deformation modes. For 2D considerations, these deformation modes are here denoted Mode I, governed by peel deformation w and peel stress σ, and Mode II, governed by shear deformation v and shear stress τ. In **Paper D** the deformation w is denoted u_{n} and v is denoted u_{s}. These stress-deformation relationships, $\sigma(w,v)$ and $\tau(w,v)$, are referred to as cohesive laws. Both loading directions and illustrative cohesive laws are shown in Fig. 1. When an adhesive layer is loaded in both Mode I and Mode II simultaneously, as shown in Fig. 1, this is denoted mixed mode loading.

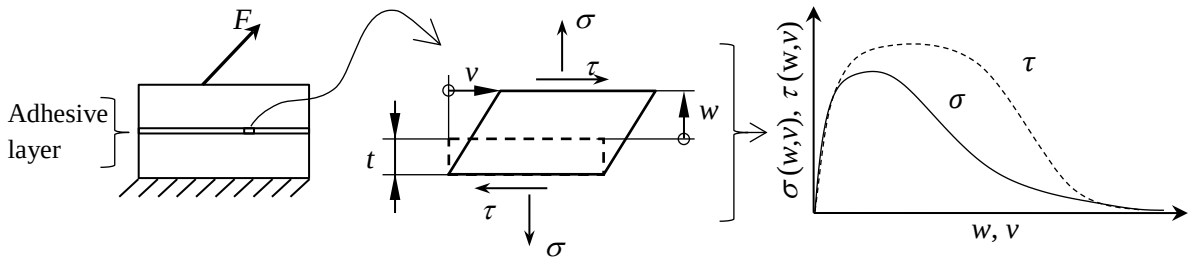

Fig. 1. Illustration of an adhesive layer with thickness, cohesive stresses (σ,τ) with work-conjugated separations (w,v) and illustrative cohesive laws.

Energy release rate

In fracture mechanics, the energy release rate (ERR) is a central concept. The ERR is denoted $\mathcal{G}$ for linear elastic fracture mechanics or, more arbitrary, J for non-linear elastic cases. By use of the ERR, the energy required to form and grow a crack in an evaluated structure is described. For a properly designed and bonded specimen, where fracture is insulated to a concentred zone, cohesive laws can be determined by measuring J and the deformations at the start of this zone. The cohesive laws are obtained as

$$\sigma = \frac{dJ}{dw}, \qquad \tau = \frac{dJ}{dv}. \tag{1}$$

Thus, by having properly designed test specimens, cohesive laws can be determined experimentally. For a properly designed, linear elastic, specimen having a small process zone $\mathcal{G}$ can replace J in Eq. (1). For a tests specimen, having a single crack tip, J or $\mathcal{G}$ is defined as the loss of potential energy $\partial\Pi$ per unit width of the specimen b, for an infinitesimal increase in crack length ∂a. For an elastic material, J can be written as

$$J = -\frac{1}{b}\frac{\partial \Pi}{\partial a} \tag{2}$$

which is derived for linear elasticity in e.g. Tada et al. (1973). For a linear elastic specimen with a single crack tip, loaded with a prescribed load F, the potential energy is given by $\Pi = S_{\mathrm{e}} - \Pi_{\mathrm{L}} = \frac{1}{2}F\Delta - F\Delta$. Here Δ denotes the load point displacement of the specimen, S_{e} denotes the strain energy and Π_{L} denotes the potential of the load. By defining the compliance $C \equiv \Delta/F$, Eq. (1) can be written

$$\mathcal{G} = \frac{F^2}{2b}\frac{\partial C}{\partial a} \tag{3}$$

which is known as the Irwing-Kies' equation, cf. Irwin and Kies (1954). By evaluating Eq. (2) under controlled displacement loading, taking the compliance of a test machine into account, one still obtain the result in Eq. (3). This shows that the ERR does not depend on the choice between prescribed displacement and load controlled testing. The definition of $\mathcal{G}$ in Eq. (3) is derived for linear elastic materials. For non-linear and linear elastic materials, J can be calculated by the use of the J-integral given by Rice (1968) and Cherepanov (1967). The J-integral is given by

$$J = \int_C \left(W \, \mathrm{d}y - T_i u_{i,x} \, dC \right) \tag{4}$$

where C denotes any counter-clockwise path surrounding the crack tip, W denotes the strain energy density of the material, **T** denotes the traction vector and **u** denotes the deformation vector. With some requirements fulfilled, J for any closed integration path is zero and thus the J-integral is path-independent. To have path independence is necessary in order to determine cohesive laws using this method. The first requirement is that W is not allowed to explicitly be dependent on the coordinate x oriented along the adhesive layer. This means that the adhesive layer needs to be uniform along its length in terms of mechanical properties, thickness and width. Furthermore, J is only valid for quasi-static loading conditions, i.e. any inertia effects must be assumed as negligible. With these requirements fulfilled, the J-integral is path-independent for any non-linear elastic material as adherends.

Test specimens

For testing adhesive layers, the two most commonly used test specimens are the double cantilever beam (DCB) and the end notch flexure (ENF) specimens. Each of these specimens consists of two adherends that are partially joined by an adhesive layer. The part of the specimen that is not joined by an adhesive layer is considered as a crack with length a and the start of the adhesive layer is denoted the crack tip.

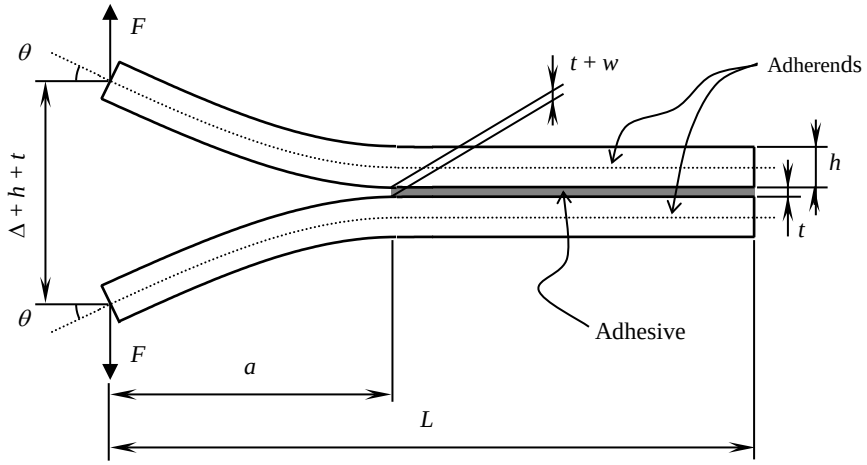

Fig. 2. Deformed DCB test specimen with out of plane width *b*.

The DCB specimen, cf. Fig. 2, is used for testing adhesive layers during pure Mode I loading. That is, where the adherends separate in the normal direction relative the surface of the adhesive layer. The DCB specimen can be loaded using applied moments or with transversal forces. The expression of J for a transversally loaded, bonded, DCB specimen is derived by Olsson and Stigh (1989) and with applied moments in Rice (1968) and Suo et al. (1992). In Nilsson (2006), J is derived to also account for large deformations by

$$J = \frac{2F}{b}\sin\theta \qquad (5)$$

where F is the applied load, θ is the load point rotation and b is the width of the adhesive layer, cf. Fig. 2. Experimental results for structural adhesives using the methods in Olsson and Stigh (1989), Rice (1968) and Suo et al. (1992) are presented in e.g. Stigh and Andersson (2000), Sørensen (2002), Andersson and Stigh (2004) and Andersson and Biel (2006).

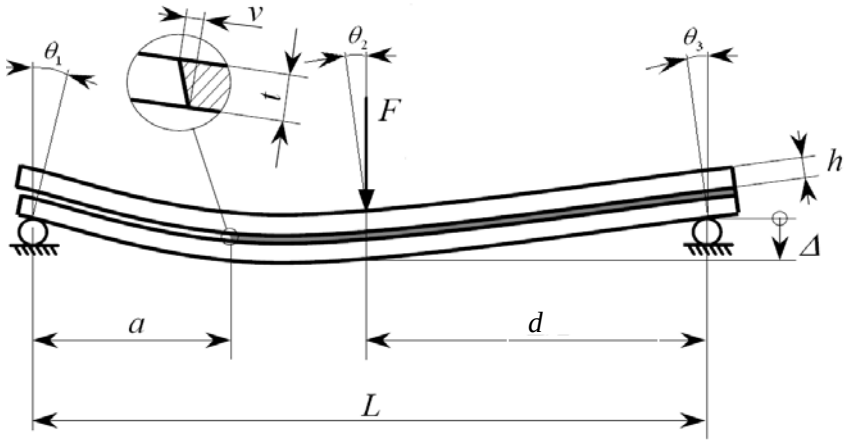

Fig. 3. Deformed ENF test specimen with out of plane width *b*.

An ENF specimen, cf. Fig. 3, is used for testing adhesive layers during an, in practice, pure Mode II loading at the crack tip. That is, where the adherends separate the adhesive in a direction along the adhesive layer. For this type of specimen, a method for calculating J for bonded specimens subjected to transversal loadings is derived in Alfredsson et al. (2002) and Alfredsson (2004). In Stigh et al. (2009), a method that allows for smaller specimen dimensions than by the method in Alfredsson et al. (2002) and Alfredsson (2004) is presented. From the work in Stigh et al. (2009), J is calculated by

$$J = \frac{F}{b}\left[\frac{d}{L}\sin\theta_1 - \sin\theta_2 + \left(1 - \frac{d}{L}\right)\sin\theta_3\right] \qquad (6)$$

where F is the applied load, θ_1, θ_2, θ_3 are rotations and d, L, and b are dimensions, cf. Fig. 3. Experimental results using transversally loaded ENF specimens with adhesives are presented in e.g. Alfredsson et al. (2002), Alfredsson (2004), Leffler et al. (2007), Stigh et al. (2009) and Walander (2009).

To determine J for a mixed mode loaded adhesive layer, a new type of specimen and testing machine is developed in **Paper D**. The concept of the set-up is based on a MMB specimen, cf. ASTM (2003), where the lever arm is replaced by two actuators that control the deformations of the specimen. The test set-up is therefore referred to as controlled mixed mode bending (CMMB). The CMMB specimen is shown in Fig. 4. Similar to the DCB and the ENF specimens, the CMMB specimen consists of two adherends that are partially joined by an adhesive layer and the part of the specimen that is not joined by an adhesive layer is considered as a crack with length a with the start of the adhesive layer denoted as the crack tip.

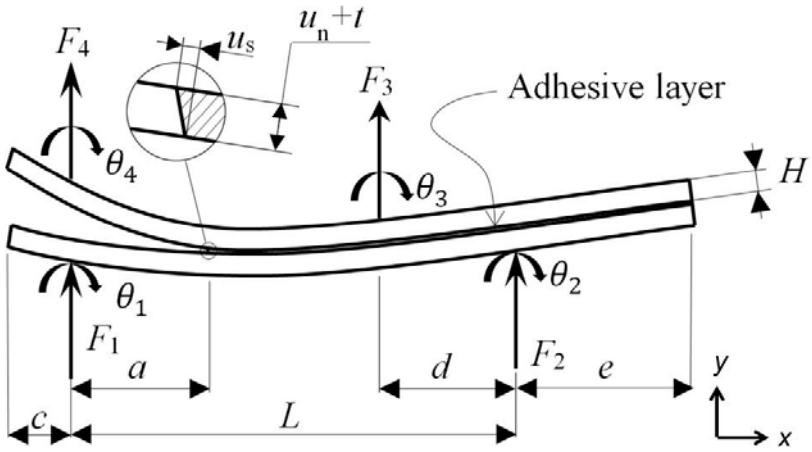

Fig. 4. Deformed CMMB specimen having an initial layer thickness t and out-of-plane width b.

The CMMB specimen is loaded with controlled displacement and the resulting loads, F_1 to F_4 are measured and defined as positive when directed upwards in Fig. 4. The resulting deformation of the adhesive layer at the crack tip is denoted u_n for peel- and u_s for shear-deformation. Clockwise rotational deformations of the adherends, corresponding to the points where the loads are applied, are denoted θ_1 to θ_4. J for the CMMB specimen is derived using the J-integral in Eq. (4). By having the overhangs c and e large enough, vertical strains at the ends of the specimen that will contribute to J can be neglected. By evaluating the specimen using Eq. (4), J is given by

$$J = \frac{1}{b}(F_1 \sin\theta_1 + F_2 \sin\theta_2 + F_3 \sin\theta_3 + F_4 \sin\theta_4)\,. \tag{7}$$

While the DCB and ENF specimens each have constant pure mode loading of the adhesive layer, the CMMB test can be regulated to control the applied deformations so that a constant mode-mixity at the crack tip is maintained. In this thesis, the mode-mixity is chosen as

$$\phi = \arctan\frac{u_\mathrm{s}}{u_\mathrm{n}} \tag{8}$$

in which $\phi = 0°$ corresponds to pure Mode I and $\phi = 90°$ correspond to pure Mode II.

Fatigue loading

Fatigue is referred to as the weakening of a material due to repetitive loading. Useful definitions in fatigue contexts are the mean stress level $\sigma_m = \frac{\sigma_\mathrm{max}+\sigma_\mathrm{min}}{2}$, the stress ratio $R_\sigma = \frac{\sigma_\mathrm{min}}{\sigma_\mathrm{max}}$ and the stress amplitude $\sigma_a = \frac{\sigma_\mathrm{max}-\sigma_\mathrm{min}}{2}$ where σ_max and σ_min refers to the maximum respective minimum stress in a repetition. Similar definitions can be constituted regarding strains and are thus denoted ϵ_m, R_ϵ and ϵ_a, respectively.

Commonly, fatigue is divided in categories, dependent on how many repetitions, i.e. load cycles, that is required to break the material. Commonly for engineering purposes, a number of cycles to failure less than approximately 10^4 cycles is referred to as low cycle fatigue (LCF), a number of cycles to failure above this level is referred to as high cycle fatigue (HCF) and for a number of cycle to failure above 10^9 cycles is referred to as very high cycle fatigue (VHCF). The first and latter are not referred to in detail in this thesis. When evaluating HCF results, the nominal stress vs. number of cycles to failure is often visualized in a semi-log plot. This representation is also referred to as S-N or Wöhler

curves. Also variants of this, where e.g. the maximum deformations are visualized against the number of cycles are presented, are sometimes also referred to as Wöhler-curves.

The fracture driven process differs between LCF and HCF. LCF is associated to structures where cyclic stress and strain amplitudes are so high that yielding occurs in the propagated fracture process zone. LEFM is thus not suitable as an evaluation method in LCF. With exception of effects such as elastic shakedown, the cyclic stress and strain amplitudes in HCF are low so that the material is to be considered cyclically loaded within an elastic range.

Not only the maximum load levels influence the fatigue life of an adhesive, but also mean stresses may influence. The influence on mean stresses is however not studied in this thesis. For a sufficiently high number of cycles to failure a material is considered to have infinite fatigue life regarding HCF. The corresponding stress and strain levels are denoted the fatigue limits of the material. A conservative method to avoid fatigue in structures is to design the structure so that no stresses exceed this fatigue limit. However, this approach gives large, and not vey optimized, structures. Instead, it is preferable to have a simulation model where the mechanical degradation of the component can be simulated. By this, the structure can be designed to be more optimized for its service life.

3. Summary of appended papers

This thesis deals with some aspects that influence the strength of adhesive layers. Each appended paper focuses on one of such aspects. Brief summaries of each paper are given below.

Paper A: *Temperature dependence of cohesive laws for an epoxy adhesive in Mode I and Mode II loading.*

This paper addresses the influence of temperature on the strength of a structural epoxy based adhesive in both Mode I and Mode II loading. The paper deals with experiments, cohesive modelling and finite element simulations. The used specimen types are the DCB and the ENF specimens. From the experiments, stress-deformation relations, i.e. cohesive laws, of the adhesive are determined for both loading modes within the temperature span -30°C to +40°C. For the Mode I experiments, the lowest temperature of the study is -40°C. **Figure A1** shows representative cohesive laws for each temperature and loading mode. All temperatures are below the glass transition temperature of the adhesive. This study is the first to report the temperature dependence of cohesive laws in Mode II loading.

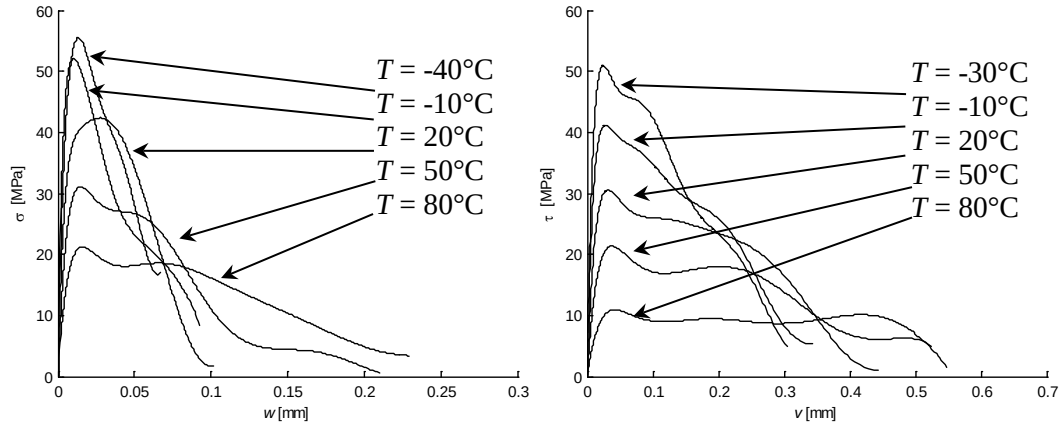

Figure A1 Representative cohesive laws for each temperature group. *Left*: Mode I. *Right*: Mode II.

From the cohesive laws, three parameters are studied in detail, namely the initial stiffness, the peak stress and the fracture energy. It is shown that all parameters, except the Mode I fracture energy, decrease with an increasing temperature for both loading modes. The Mode I, the fracture energy is shown to be independent of the temperature within the evaluated temperature span.

Using the experimental results, finite element analyses are performed. By modelling the DCB and the ENF specimens with implemented cohesive laws, the simulated force vs. load point deformation relationships are compared to the experimentally measured relationships. Good fits give confidence in the evaluated cohesive laws. Two types of models of the cohesive laws are used in the simulations. The most advanced model mimics the actual shape of the cohesive law at each evaluated temperature and loading mode. This model is denoted shape-mimicking cohesive law. The other model is a bilinear law that is constructed by the three evaluated parameters at each loading mode. By performing regression analyses of these parameters with respect to the temperature, any temperature within the evaluated span can be simulated. The shape-mimicking model yields the best correspondence to the experimental results. However, only the evaluated temperatures can be simulated using these results.

Paper B: *High cycle fatigue crack growth in Mode I of adhesive layers - Modelling, simulation and experiments.*

This paper focuses on high cycle fatigue of two adhesive layers subjected to pure Mode I loading. The studied adhesive layers differ in their thicknesses and mechanical properties. One adhesive is a relatively stiff rubber based adhesive having a nominal layer thickness of 0.3 mm and the other is a relatively soft polyurethane (PUR) based adhesive having a nominal layer thickness of 1.0 mm. The aim with the work is to identify a suitable Mode I damage evolution law for large-scale simulation of built-up structures that can be used for any adhesive system.

The work contains experiments, modelling and finite element simulations. In the experimental study, a SEM study of one of the adhesives and fatigue tests of both adhesives are performed. The cohesive laws of both adhesive layers are determined using DCB specimens. Compliance calibrations and fatigue tests are performed using identical experimental set-ups for both adhesives, although the specimen dimensions differ between the two adhesive systems. For this, a test rig is designed for testing up to six DCB specimens simultaneously. The fatigue tests are performed under controlled displacement, Δ, with a deformation ratio $R_\Delta = \frac{\Delta_{\min}}{\Delta_{\max}} = 0.1$ where $\Delta_{\max} > 0$. In the tests, we monitor the maximum and minimum values of the load and the displacement at each recorded load cycle. Together with the results of the compliance calibration, the energy release rate and the crack length is calculated. From the experimental results, it is shown that the energy release rate decreases monotonically with respect to the number of cycles during the entire experiment and that no steady state in energy release rate is present for any of evaluated specimens and adhesives.

From the experimental results, parameters to model the experiments using a fracture mechanics approach based on Paris' law are identified for both adhesives. However, a fracture mechanics approach assumes the crack tip to be sharp and pre-cracked. This means that the damage initiation phase is ignored. Damage initiation can constitute a substantial part of the life of structures. Since it is desirable to model the damage initiation phase, a damage mechanics model is developed. The damage mechanics model is implemented as a cohesive zone model.

In high cycle fatigue, it is not computationally efficient to follow the entire evolution of stress during each load cycle. Therefore, the evolution of the maximum stress in each load cycle is analysed. This stress is assumed to be directly related to the damage driving stress σ_{F} in the cohesive zone. Damage D is assumed to grow from the initial value $D = 0$ with the number of load cycles N according to

$$\frac{\mathrm{d}D}{\mathrm{d}N} = \alpha \left[\frac{<\sigma_{\mathrm{F}} - \sigma_{\mathrm{th}}>}{\sigma_0}\right]^{\beta} \qquad \text{(B1)}$$

where σ_{th}, α and β are the only material parameters and σ_0 is a normalization constant. A Macaulay bracket $<\cdot> = (\cdot + |\cdot|)/2$ indicates that only stresses larger than σ_{th} contribute to the damage evolution. Numerically, the FE-problem is solved as a relaxation problem where the time parameter is represented by the number of load cycles N. This implies that the model lacks the details of the loading ratio and the loading frequency. In turn, this implies that that the material parameters need to be determined for a fixed load ratio and loading frequency and that only these configurations can be simulated if no interpolation and/or further assumptions on the parameters are done. In the FE-solution, large time steps can be allowed to further speed-up the analysis. A methodology to determine the material parameters is presented.

Since adhesive layers are much more compliant than the adherend materials, adhesive layers are considered to be under a state of uniaxial strain. For 3D considerations, the equivalent stress σ_{F} is calculated as the largest principal stress,

$$\sigma_{\mathrm{F}} = \max(\sigma_1, \sigma_2, \sigma_3) \tag{B2}$$

in which the principal stresses are calculated by the stress components in the adhesive layer:

$$\sigma_{xx} = \frac{E(1-\nu)}{(1+\nu)(1-2\nu)}\varepsilon_{xx}, \quad \sigma_{yy} = \frac{E\nu}{(1+\nu)(1-2\nu)}\varepsilon_{xx}, \quad \sigma_{zz} = \frac{E\nu}{(1+\nu)(1-2\nu)}\varepsilon_{xx},$$

$$\sigma_{xy} = 2G\varepsilon_{xy}, \qquad \sigma_{xz} = 2G\varepsilon_{xz}, \qquad \sigma_{\mathrm{yz}} = 0. \tag{B3}$$

In this equation E denotes the Young's modulus, ν denotes the Poission's ratio and $G = \frac{E}{2(1+\nu)}$ denotes the shear modulus for the adhesive, respectively. For the evaluated adhesive layers, configurations and load parameters, simulations using the damage mechanics model show a very good agreement with the experimental results for both evaluated adhesive layers. Thus, the model is capable of reproducing experimental behaviours of the studied adhesives.

A convergence study concerning the influence of the time steps and the mesh size are performed.

Paper C: *Fatigue life of adhesively bonded structures.*

This paper is a continuation of the study in **Paper B**. While the damage model and experiments in **Paper B** only focuses on Mode I loading, this study considers fatigue damage in a more complex loading of a real engineering component. The study contains simulations, experiments and modelling. A bonded automotive component is used to experimentally generate mixed mode loading of an adhesive layer. The component is loaded under displacement control with a displacement ratio and loading rate identical to the ones in **Paper B**. The stiffness of the specimen decreases with an increase in loading cycles. By defining fracture of a specimen as the moment when 80 % of the initial stiffness remains, a variant of a Wöhler curve is constructed by the experimental results, cf. Fig. C1.

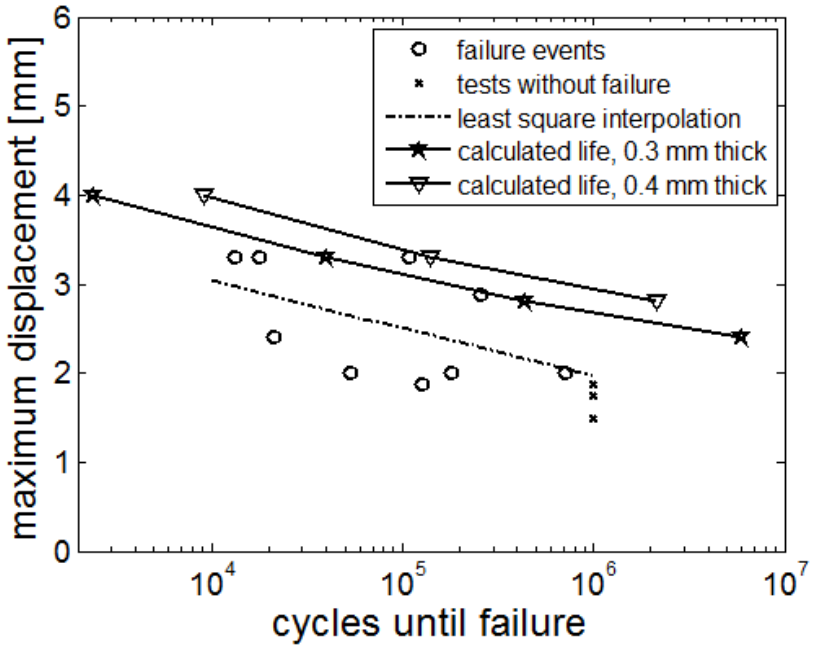

Figure C1 Representation of the experimental results together with calculated fatigue life.

As the studied component is loaded under controlled deformation with a deformation ratio $R_\Delta = \frac{\Delta_{\min}}{\Delta_{\max}} = 0.1$ for $\Delta_{\max} > 0$, the reaction force is expected to always be positive. However, yielding of the specimen occurs during the application of the first load cycle. This results in a negative force at $\Delta_{\min}$. Due to this, the force range is studied instead, cf. Fig. C2.

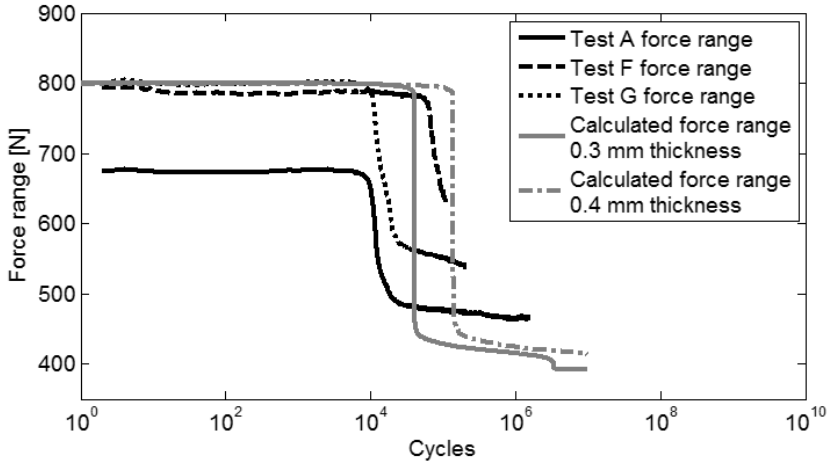

Figure C2 Experimental results of force range compared with results from simulations

The bonded structure is simulated using the same damage law as in **Paper B** in which the stress components of the adhesive layer are calculated identically. The material parameters for the damage law obtained in **Paper B** are used in the simulations of the component. However, the equivalent fatigue stress σ_F is calculated differently. In **Paper B**, σ_F is calculated by the maximum principal value of the stress components, Eq. (B3). However, comparisons of the relation between the reaction force vs. the number of load cycles between the experiments and simulations show substantial mismatch by using the stress measure in **Paper B**. An alternative stress measure is therefore developed. This stress

measure has to conform with the maximum principal stress in Mode I loading. The suggested stress measure is

$$\sigma_F = C\sqrt{\frac{2}{3}(1+\nu)\sigma_{\mathrm{VM}}^2 + 3(1-2\nu)\sigma_{\mathrm{H}}^2} \qquad \text{(C1)}$$

where

$$\sigma_{\mathrm{H}} = \frac{\sigma_1+\sigma_2+\sigma_3}{3} \text{ and } \sigma_{\mathrm{VM}} = \sqrt{\frac{(\sigma_1-\sigma_2)^2+(\sigma_2-\sigma_3)^2+(\sigma_3-\sigma_1)^2}{2}} \qquad \text{(C2)}$$

respectively, denote the hydrostatic (σ_{H}) and the von Mises stress (σ_{VM}). For $C = 1$, Eq. (C1) is derived by Lemaitre (1985). Here, the constant C is chosen so that σ_{F} conforms with the maximum principal stress in pure Mode I loading. This gives

$$C = (1-\nu)/\sqrt{(1-2\nu)(1-\nu^2)}\,. \qquad \text{(C3)}$$

For the studied adhesive $\nu = 0.45$ which yields $C \approx 1.95$. Using the suggested stress measure, a good agreement between the experimental results and the simulations is obtained concerning the force range and life.

The two counter-parts of the bonded structure are manufactured using cold forging. By this, they are not perfectly parallel or in shape with respect to each other. This makes the measured adhesive thickness to vary at different point at each specimen. The aimed adhesive thickness is 0.3 mm but the mean value in thickness of the most critical part of the structure is determined to 0.4 mm considering all specimens. In order to investigate the influence of the mechanical strength due to this variation, simulations are performed using both adhesive thicknesses. The predictions by the simulation model for the two thicknesses are included in the Wöhler curve. Both models give an estimated relative error in fatigue life, concerning the applied deformation that is less or equal to 50 % as compared to the experimental results. This extent in error is in relation to the scatter in experimental results and is thus judged as acceptable.

In order to give confidence to the simulation results, convergence studies concerning the mesh size and time increment are performed.

Paper D: *Controlled mixed-mode bending tests to determine cohesive laws of structural adhesive layers.*

This paper addresses the dependency of mode-mix on the strength of an adhesive layer. The work consists of experiments and models. While frequently used mixed mode specimens for testing adhesive layers gives a non-constant mode-mix ratio during an experiment, an experimental set-up to evaluate adhesive layers under a controlled and constant mixed mode ratio is presented. The experimental set-up is similar to a MMB set-up but instead of a lever arm, two servo-controlled actuators are used to regulate the loadings of the specimen. The actuators are regulated so that a constant mode-mix ratio is ensured. The mode-mix ratio definition used in this study is based on the normal and shear deformations at the crack tip of the specimen.

By comparison, the specimen design in the experiments is similar to the design used in a MMB standard experiment, ASTM (2003), but it is significantly larger. The reason is that the specimen needs to be large enough to be able to use the J-integral in the evaluations. The studied adhesive in this work is identical to, and is given the same nominal layer thickness as, in **Paper A**. All experiments are

performed at room temperature. As the CMMB specimen is designed to fulfil all requirements for J to be path-independent, the pure Mode I and pure Mode II cohesive laws from the CMMB experiments give results that correspond well with the results in **Paper A**.

J-curves vs. normal and shear deformations are obtained experimentally at both positive and negative mode-mixes. From the J-curves, the point of fracture and thereby the fracture energy is determined. By the experimental results, a fracture envelope is presented in which the fracture energy of the studied adhesive is presented against the mode-mix angle $\phi = \arctan(\frac{u_s}{u_n})$. This envelope is shown in Figure D1 where triangles represent the CMMB results. From this figure, it is shown that the fracture envelope of the studied adhesive is symmetrical with respect to the mode-mix angle.

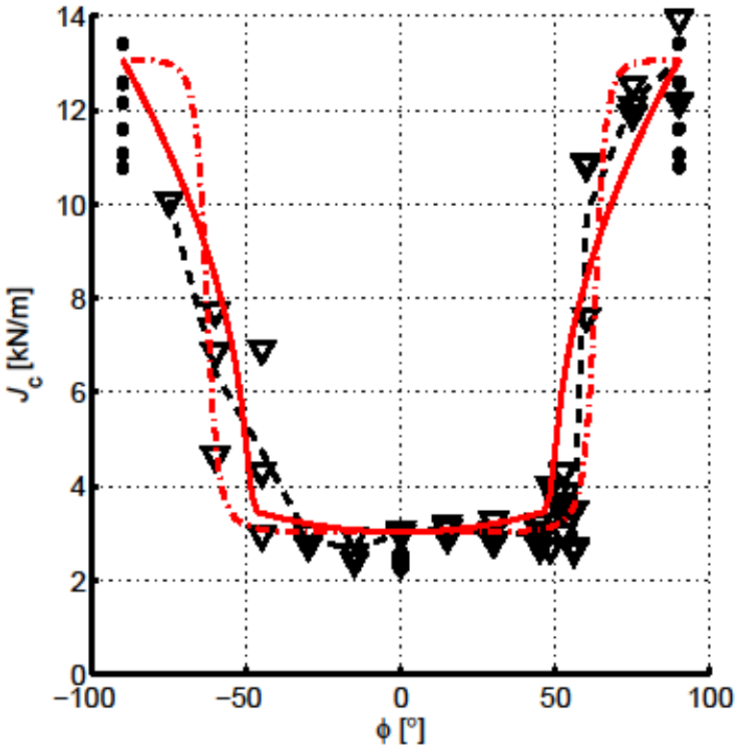

Figure D1 Fracture envelope. Experimental results compared to predictions of the two shape functions. *Marks*: Experimental results. *Curves*: Predictions.

Using the experimental results, a separation based potential model is developed. The potential model is a modification of a model developed by Salomonsson and Andersson (2010). Two variants of this modified potential model are presented. One variant is developed to allow peel stress in the adhesive layer during a pure Mode II deformation while the other variant prevents these stresses. The developed potential and its variants are compared with the experimental results of the J vs. resultant displacement $u_{\text{res}} = \sqrt{u_n^2 + u_s^2}$. From the potential model, the predicted fracture energy by the potential model is determined as a function of the mode-mix angle. These predictions are included in Fig. D1. The solid red curve corresponds to the variant where peel stress during a pure Mode II loading is allowed. The dashed curve corresponds to the variant of the potential model where this peel stress is prevented. For the present adhesive, both models are shown to be able to adapt to the experimental results.

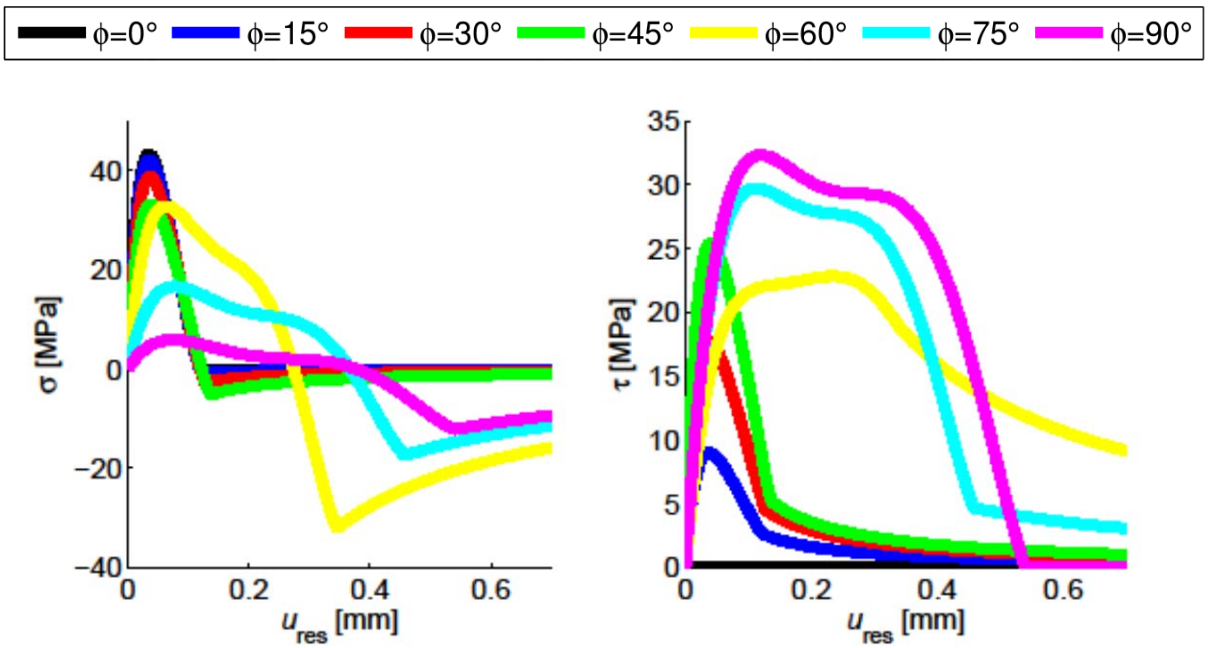

Figure D2 Prediction of cohesive stresses by the potential model vs. the resultant deformation. *Left*: peel stress. *Right*: shear stress. Model with peel stress in pure shear loading.

From the potential models, cohesive laws of the adhesive layer, for any deformations, are obtained. For the variant where peel stress during a pure Mode II loading is allowed, the cohesive laws are presented in Figure D2.

4. Concluding remarks and suggested future work

The mechanical behaviour of adhesives, considering influences of the aspects *temperature*, *mixed mode loading*, *fatigue* and *mixed mode fatigue loading*, are studied. The experiments in all of the four studies are evaluated by a fracture mechanical approach, often by use of non-linear theory. By the used methods, cohesive laws, i.e. stress-deformation relationships of the studied adhesives are obtained.

Each study presents experimental results and each study also presents models that can be used to describe the influence of the aspects on the cohesive laws numerically, e.g. by using the finite element method. All these models, except for the model in **Paper D**, are implemented in a commercial finite element software and the results of the FE-simulations correspond well with the experimental results.

Short highlights of the results of the studies are presented below.

The study in **Paper A** is the first study in the open literature to report the temperature dependence on cohesive laws of a structural adhesive in a Mode II loading. By these results, a finite element model is developed that can be used for simulations of pure mode loading at any temperature in the evaluated temperature span −30 °C to +80 °C. The FE-model is shown to give good agreement reproducing the experimental results.

Paper B, considers high cycle fatigue of two adhesive systems subjected to a pure Mode I loading. The used specimen type is the DCB specimen. A threshold value in stress is identified below which fatigue damage is not accumulated. By the experimental results, a damage evolution law is suggested for modelling fatigue of the adhesives. A convergence study is performed considering the choice of element size and time increment in the analysis. The present paper shows an inability to capture the constraining effects of the adherends using the Paris' law approach. Thus, the Paris' law properties of

an adhesive layer are not expected to be transferable to joints with adherends having different mechanical properties.

Paper C considers high cycle fatigue of a component subjected to a multi-axial fatigue loading. For the same damage evolution law and its parameters as in **Paper B**, a stress measure is suggested that is shown to be suitable for both the model in **Paper B** and also for a multi-axial loading case.

In **Paper D**, a new experimental set-up is presented for investigating strength of adhesives during a mixed mode loading. By considering the mode-mix ratio in terms of displacements at the crack tip of the specimen, the set-up enables loading with a constant mode-mix ratio. Thus, an experimental set-up for controlled mixed mode tests is presented. Experiments are performed at various mode-mix angles and for each experiment, J is determined. Two variants of a potential model are able to sufficiently describe the experimental results of J for all evaluated mode-mixes is presented. This potential model is used for determine the cohesive stresses of the evaluated adhesive.

As for suggested future work, a FE-implantation of the potential model in **Paper D** is suggested by the author. Further, the author suggests complementing the results from **Paper B** and **Paper C** with an experimental fatigue study performed in Mode II loading. As a suggestion, by using the ENF specimen.

All presented studies each focuses on one individual aspect having influence on the cohesive laws. The suggested models in each paper thus only describe one aspect respectively. Under the condition that the same adhesive and thickness is used, it could be useful to derive a model that could describe two or more aspects simultaneously. As an example, the influence on temperature could be linked to the potential model in **Paper D**.

5. References

Abdel Wahab, M. M., Hilmy, I., Ashcroft, I. A., & Crocombe, A. D. (2010a). Evaluation of fatigue damage in adhesive bonding: part 1: bulk adhesive. Journal of Adhesion Science and Technology, 24(2), 305-324.

Abdel Wahab, M. M., Hilmy, I., Ashcroft, I. A., & Crocombe, A. D. (2010b). Evaluation of fatigue damage in adhesive bonding: part 2: single lap joint. Journal of Adhesion Science and Technology, 24(2), 325-345.

Alfredsson, K. S. (2004). On the instantaneous energy release rate of the end-notch flexure adhesive joint specimen. International Journal of Solids and Structures, 41(16), 4787-4807.

Alfredsson, K. S., Biel, A., & Leffler, K. (2002). An experimental method to determine the complete stress-deformation relation for a structural adhesive layer loaded in shear. In Proceedings of the 9th international conference on the mechanical behaviour of materials, Geneva, Switzerland.

Álvarez, D., Blackman, B. R. K., Guild, F. J., Kinloch, A. J., Taylor, A. C., & Osiyemi, S. Mixed-Mode Fracture in Adhesively-Bonded Joints. 36th Annual Meeting of The Adhesion Society, Hilton Daytona Beach, Daltona, FL, USA.

Andersson, T., & Biel, A. (2006). On the effective constitutive properties of a thin adhesive layer loaded in peel. International Journal of Fracture, 141(1-2), 227-246.

Andersson, T., & Stigh, U. (2004). The stress–elongation relation for an adhesive layer loaded in peel using equilibrium of energetic forces. International Journal of Solids and Structures, 41(2), 413-434.

ASTM Standard, (2003). Standard test method for mixed mode I-mode II interlaminar fracture of unidirectional fiber-reinforced polymer matrix composites, D 6671-01. *Annual Book of ASTM Standards*, *15*, 400-411.

Atsu, S. S., Kilicarslan, M. A., Kucukesmen, H. C., & Aka, P. S. (2006). Effect of zirconium-oxide ceramic surface treatments on the bond strength to adhesive resin. The Journal of prosthetic dentistry, 95(6), 430-436.

Banea MD, da Silva LFM, Campilho RDSG (2012) Mode II fracture toughness of adhesively bonded joints a function of temperature: Experimental and numerical study. J Adh 88:534-551

Benzeggagh, M. L., & Kenane, M. (1996). Measurement of mixed-mode delamination fracture toughness of unidirectional glass/epoxy composites with mixed-mode bending apparatus. Composites Science and Technology, 56(4), 439-449.

Biel, A., Walander, T., & Stigh, U. (2012). Influence of Edge-boundaries on the Cohesive Behaviour of an Adhesive Layer. In ASME 2012 International Mechanical Engineering Congress and Exposition (pp. 507-511). American Society of Mechanical Engineers.

Cadenaro, M., Breschi, L., Rueggeberg, F. A., Agee, K., Di Lenarda, R., Carrilho, M., Tay, F. & Pashley, D. H. (2009). Effect of adhesive hydrophilicity and curing time on the permeability of resins bonded to water vs. ethanol-saturated acid-etched dentin. Dental materials, 25(1), 39-47.

Carlberger T, Biel A, Stigh U. (2009) Influence of temperature and strain rate on cohesive properties of a structural epoxy adhesive. Int J Fract155:155-166

Chai, H. (2004). The effects of bond thickness, rate and temperature on the deformation and fracture of structural adhesives under shear loading. International journal of fracture, 130(1), 497-515.

Charalambides, M., Kinloch, A. J., Wang, Y., & Williams, J. G. (1992). On the analysis of mixed-mode failure. International Journal of Fracture, 54(3), 269-291.

Cherepanov, G. P. (1967). The propagation of cracks in a continuous medium. Journal of Applied Mathematics and Mechanics, 31(3), 503-512.

Cho, J. U., Kinloch, A., Blackman, B., Sanchez, F. R., & Han, M. S. (2012). High-strain-rate fracture of adhesively bonded composite joints in DCB and TDCB specimens. International Journal of Automotive Technology, 13(7), 1127-1131.

Conroy, M., Ivankovic, A., Karac, A., & Williams, J. G. (2013). MODE-MIXITY IN BEAM LIKE GEOMETRIES: GLOBAL PARTITIONING WITH COHESIVE ZONES. In 36th Annual Meeting of The Adhesion Society, Hilton Daytona Beach, Daltona, FL, USA.

Crocombe, A. D., Hua, Y. X., Loh, W. K., Wahab, M. A., & Ashcroft, I. A. (2006). Predicting the residual strength for environmentally degraded adhesive lap joints. International Journal of Adhesion and Adhesives, 26(5), 325-336.

Evans, A. G., Hutchinson, J. W., & Wei, Y. (1999). Interface adhesion: effects of plasticity and segregation. Acta Materialia, 47(15), 4093-4113.

Fuller, K. N. G., & Tabor, D. F. R. S. (1975). The effect of surface roughness on the adhesion of elastic solids. In Proceedings of the Royal Society of London A: Mathematical, Physical and Engineering Sciences (Vol. 345, No. 1642, pp. 327-342). The Royal Society.

Graner Solana, A. G., Crocombe, A. D., & Ashcroft, I. A. (2010). Fatigue life and backface strain predictions in adhesively bonded joints. International Journal of Adhesion and Adhesives, 30(1), 36-42.

Högberg, J. L. (2006). Mixed mode cohesive law. International Journal of Fracture, 141(3-4), 549-559.

Högberg, J. L., Sørensen, B. F., & Stigh, U. (2007). Constitutive behaviour of mixed mode loaded adhesive layer. International Journal of Solids and Structures, 44(25), 8335-8354.

Irwin, GR, Kies, JA (1954) Critical energy rate analysis of fracture strength. Weld J Res Suppl 33: pp. 193-198

Ji, G., Ouyang, Z., Li, G., Ibekwe, S., & Pang, S. S. (2010). Effects of adhesive thickness on global and local Mode-I interfacial fracture of bonded joints. International Journal of Solids and Structures, 47(18), 2445-2458.

Khoramishad, H., Crocombe, A. D., Katnam, K. B., & Ashcroft, I. A. (2010a). Predicting fatigue damage in adhesively bonded joints using a cohesive zone model. International Journal of fatigue, 32(7), 1146-1158.

Khoramishad, H., Crocombe, A. D., Katnam, K. B., & Ashcroft, I. A. (2010b). A generalised damage model for constant amplitude fatigue loading of adhesively bonded joints. International Journal of Adhesion and Adhesives, 30(6), 513-521.

Kinloch, A. J., & Osiyemi, S. O. (1993). Predicting the fatigue life of adhesively-bonded joints. The Journal of adhesion, 43(1-2), 79-90.

Kinloch, A. J., & Shaw, S. J. (1981). The fracture resistance of a toughened epoxy adhesive. The Journal of Adhesion, 12(1), 59-77.

Klarbring, A. (1991). Derivation of a model of adhesively bonded joints by the asymptotic expansion method. International Journal of Engineering Science, 29(4), 493-512.

Lane, M., Dauskardt, R. H., Vainchtein, A., & Gao, H. (2000). Plasticity contributions to interface adhesion in thin-film interconnect structures. Journal of materials research, 15(12), 2758-2769.

Lee, D. B., Ikeda, T., Miyazaki, N., & Choi, N. S. (2004). Effect of bond thickness on the fracture toughness of adhesive joints. Journal of engineering materials and technology, 126(1), 14-18.

Lee, D. G., Kim, K. S., & Im, Y. T. (1991). An experimental study of fatigue strength for adhesively bonded tubular single lap joints. The Journal of Adhesion, 35(1), 39-53.

Leffler, K., Alfredsson, K. S., & Stigh, U. (2007). Shear behaviour of adhesive layers. International Journal of Solids and Structures, 44(2), 530-545.

Lemaitre, J. (1985). A continuous damage mechanics model for ductile fracture. Journal of Engineering Materials and Technology, 107(1), 83-89.

Li R, Jiao J (2000) The effects of temperature and aging on Young's moduli of polymeric based flexible substrates. Proc. Int. Soc. Opt. Eng. 1999, 2000

Lucena-Martín, C., González-López, S., & de Mondelo, J. M. N. R. (2001). The effect of various surface treatments and bonding agents on the repaired strength of heat-treated composites. The Journal of prosthetic dentistry, 86(5), 481-488.

Lundsgaard-Larsen, C., Sørensen, B. F., Berggreen, C., & Østergaard, R. C. (2008). A modified DCB sandwich specimen for measuring mixed-mode cohesive laws. Engineering Fracture Mechanics, 75(8), 2514-2530.

Marzi, S., Hesebeck, O., Brede, M., & Kleiner, F. (2009). A rate-dependent cohesive zone model for adhesively bonded joints loaded in mode I. Journal of Adhesion Science and Technology, 23(6), 881-898.

Marzi, S., Hesebeck, O., Brede, M., Nagel, C., Biel, A., Walander, T., & Stigh, U. (2014). Effects of the bond line thickness on the fracture mechanical behaviour of structural adhesive joints. In Proceedings of the Annual Meeting of the Adhesion Society 2014. Adhesion Society.

May, M., Hesebeck, O., Marzi, S., Böhme, W., Lienhard, J., Kilchert, S., Brede, M. & Hiermaier, S. (2015). Rate dependent behavior of crash-optimized adhesives–Experimental characterization, model development, and simulation. Engineering Fracture Mechanics, 133, 112-137.

Mostovoy, S., Ripling, E. J., & Bersch, C. F. (1971). Fracture toughness of adhesive joints. The Journal of Adhesion, 3(2), 125-144.

Nilsson, F. (2006). Large displacement aspects on fracture testing with double cantilever beam specimens. International journal of fracture, 139(2), 305-311.

Olsson, P., & Stigh, U. (1989). On the determination of the constitutive properties of thin interphase layers—an exact inverse solution. International Journal of Fracture, 41(4), R71-R76.

Pardoen, T., Ferracin, T., Landis, C. M., & Delannay, F. (2005). Constraint effects in adhesive joint fracture. Journal of the Mechanics and Physics of Solids, 53(9), 1951-1983.

Park, K., & Paulino, G. H. (2011). Cohesive zone models: a critical review of traction-separation relationships across fracture surfaces. Applied Mechanics Reviews, 64(6), 060802.

Parvatareddy, H., & Dillard, D. A. (1999). Effect of mode-mixity on the fracture toughness of Ti-6Al-4V/FM-5 adhesive joints. International journal of fracture, 96(3), 215-228.

Persson, B. N. J., & Tosatti, E. (2001). The effect of surface roughness on the adhesion of elastic solids. The Journal of Chemical Physics, 115(12), 5597-561

Persson, B. N. J., Albohr, O., Tartaglino, U., Volokitin, A. I., & Tosatti, E. (2005). On the nature of surface roughness with application to contact mechanics, sealing, rubber friction and adhesion. Journal of Physics: Condensed Matter, 17(1), R1.

Pirondi, A., & Moroni, F. (2009). An investigation of fatigue failure prediction of adhesively bonded metal/metal joints. International Journal of Adhesion and Adhesives, 29(8), 796-805.

Pirondi, A., & Nicoletto, G. (2004). Fatigue crack growth in bonded DCB specimens. Engineering fracture mechanics, 71(4), 859-871.

Rice, J. R. (1968). A path independent integral and the approximate analysis of strain concentration by notches and cracks. Journal of applied mechanics, 35(2), 379-386.

Sadr, A., Shimada, Y., & Tagami, J. (2007). Effects of solvent drying time on micro-shear bond strength and mechanical properties of two self-etching adhesive systems. Dental materials, 23(9), 1114-1119.

Salomonsson, K. E., & Andersson, T. J. (2010). Weighted Potential Methodology for Mixed Mode Cohesive Laws. In MECOM DEL BICENTENARIO: CILAMCE 2010 (XXXI Iberian-Latin-American Congress on Computational Methods in Engineering) and MECOM 2010 (IX Argentine Congress on Computational Mechanics and II South American Congress on Computational Mechanics). Buenos Aires, Argentina, 15-18 November 2010 (pp. 8355-8374). Asociación Argentina de Mecánica Comptacional.

Schmidt, P. (2008). Modelling of adhesively bonded joints by an asymptotic method. International Journal of Engineering Science, 46(12), 1291-1324.

Schnell, R., Stamm, M., & Creton, C. (1998). Direct correlation between interfacial width and adhesion in glassy polymers. Macromolecules, 31(7), 2284-2292.

Sørensen, B. F. (2002). Cohesive law and notch sensitivity of adhesive joints. Acta Materialia, 50(5), 1053-1061.

Sørensen, B. F., & Jacobsen, T. K. (2009). Characterizing delamination of fibre composites by mixed mode cohesive laws. Composites science and technology, 69(3), 445-456.

Sørensen, B. F., & Kirkegaard, P. (2006). Determination of mixed mode cohesive laws. Engineering fracture mechanics, 73(17), 2642-2661.

Stamoulis, G., Carrère, N., Cognard, J. Y., Davies, P., & Badulescu, C. (2014). On the experimental mixed-mode failure of adhesively bonded metallic joints. International Journal of Adhesion and Adhesives, 51, 148-158.

Stigh, U., & Andersson, T. (2000). An experimental method to determine the complete stress-elongation relation for a structural adhesive layer loaded in peel. European Structural Integrity Society, 27, 297-306.

Stigh, U., Alfredsson, K. S., & Biel, A. (2009, January). Measurement of cohesive laws and related problems. In ASME 2009 International Mechanical Engineering Congress and Exposition (pp. 293-298). American Society of Mechanical Engineers.

Suliman, A. H. A., Swift, E. J., & Perdigao, J. (1993). Effects of surface treatment and bonding agents on bond strength of composite resin to porcelain. The Journal of prosthetic dentistry, 70(2), 118-120.

Suo, Z., Bao, G., & Fan, B. (1992). Delamination R-curve phenomena due to damage. Journal of the Mechanics and Physics of Solids, 40(1), 1-16.

Tada, H. (1973). Paris, PC and Irwin, GR. The stress analysis of cracks handbook, 27-1.

Uehara, K., & Sakurai, M. (2002). Bonding strength of adhesives and surface roughness of joined parts. Journal of materials processing technology, 127(2), 178-181.

Vieira, L. C. C., Araújo, É., & Monteiro Júnior, S. (2004). Effect of different ceramic surface treatments on resin microtensile bond strength. Journal of Prosthodontics, 13(1), 28-35.

Wahab, M. A., Ashcroft, I. A., Crocombe, A. D., & Smith, P. A. (2002). Numerical prediction of fatigue crack propagation lifetime in adhesively bonded structures. International journal of fatigue, 24(6), 705-709.

Walander, T. (2009). System for measurement of cohesive laws. M.Sc. Thesis, University of Skövde

Wingfield, J. R. J. (1993). Treatment of composite surfaces for adhesive bonding. International journal of adhesion and adhesives, 13(3), 151-156.

Yang, Q. D., & Thouless, M. D. (2001a). Mixed-mode fracture analyses of plastically-deforming adhesive joints. International Journal of Fracture, 110(2), 175-187.

Yang, Q. D., Thouless, M. D., & Ward, S. M. (2001b). Elastic–plastic mode-II fracture of adhesive joints. International Journal of Solids and Structures, 38(18), 3251-3262

Paper A:
Walander, T., Biel, A., & Stigh, U. (2013). Temperature dependence of cohesive laws for an epoxy adhesive in Mode I and Mode II loading. International Journal of Fracture, 183(2), 203-221.

Paper B:
Eklind, A., Walander, T., Carlberger, T., & Stigh, U. (2014). High cycle fatigue crack growth in Mode I of adhesive layers: modelling, simulation and experiments. International Journal of Fracture, 190(1-2), 125-146

Paper C:
T. Walander, A. Eklind, T. Carlberger, U. Stigh, A. Rietz (2015). Fatigue life of adhesively bonded structures. Submitted.

Paper D:
T. Walander, S. Marzi, O. Hesebeck (2015). Controlled mixed-mode bending tests to determine cohesive laws of structural adhesive layers. Submitted.